Energy for Sustainable Development 23 (2014) 99–109

Contents lists available at ScienceDirect

Energy for Sustainable Development

The effects of fuel type and stove design on emissions and efficiency of natural-draft semi-gasifier biomass cookstoves

Jessica Tryner, Bryan D. Willson, Anthony J. Marchese *

Department of Mechanical Engineering, Colorado State University, 1374 Campus Delivery, Fort Collins, CO 80523-1374, USA

ARTICLE INFO

Article history:
Received 9 April 2014
Revised 7 July 2014
Accepted 21 July 2014
Available online xxxx

Keywords:
Biomass combustion
Cookstoves
Top-lit up-draft gasifier
Carbon monoxide emissions
Particulate matter emissions
Cookstove design

ABSTRACT

To assess the effects of stove design and fuel type on efficiency and emissions, five configurations of natural-draft, top-lit up-draft (TLUD) semi-gasifier cookstoves were tested with two biomass fuels. An energy balance model was developed using measured temperature data to identify the major sources of efficiency loss. Emissions and efficiency varied substantially with stove design and fuel type, and transient increases in CO emission correlated with refueling. The highest measured thermal efficiency was 42%. The lowest CO and PM emissions were 0.6 g MJd^{-1} and 48 g MJd^{-1}. These results fall within Tier 3 for high-power efficiency and emissions and suggest that development of a Tier 4 natural-draft semi-gasifier cookstove is possible. The energy balance illustrates that up to 60% of the energy input as fuel can remain as char once the fuel has gasified. This result suggests that both thermal and overall efficiencies should be calculated when evaluating TLUD cookstoves.

Introduction

It is estimated that forty percent of the global population relies on combustion of solid biomass fuel to fulfill some or all of their household energy needs (Bonjour et al., 2013). The majority of this population uses biomass cookstoves that are characterized by incomplete combustion. Public health researchers have linked exposure to the carbon monoxide (CO) and particulate matter (PM) emissions from incomplete combustion of solid biomass to numerous health effects such as acute lower respiratory infections and chronic obstructive pulmonary disease (Bruce et al., 2006). Some have suggested that a transition to affordable liquid or gaseous cooking fuels would be necessary to completely eliminate these health impacts (Goldemberg et al., 2004). However, even if a transition to liquid or gaseous fuels is ultimately necessary, such a transition would take many years to accomplish given the size and geographic distribution of the affected population. Consequently, a substantial fraction of the global population is expected to continue cooking with solid biomass fuel for the foreseeable future (Rehfuess et al., 2006).

In recent years, designers of household cookstoves have focused on improving efficiency and reducing emissions to mitigate health impacts associated with the use of solid biomass fuel. Rocket elbow cookstoves have been shown to reduce emissions by up to 60% compared to a three-stone fire (Jetter and Kariher, 2009). However, ongoing public health research is expected to reveal that greater emission reductions are needed to substantially reduce health risks (Smith and Peel, 2010).

Semi-gasifier cookstoves have been shown to be the lowest-emitting type of solid biomass cookstove based on emission measurements taken in the laboratory (Jetter and Kariher, 2009; Jetter et al., 2012). Most of the semi-gasifier cookstoves that have been developed utilize the top-lit up-draft (TLUD) design (Anderson and Reed, 2007). In the TLUD design, solid fuel is batch fed into the combustion chamber and ignited from the top as shown in Fig. 1. Consumption of the fuel proceeds downward (Reed and Larson, 1996). A primary air source that enters at the bottom of the fuel bed results in partial oxidization of the fuel into CO, H_2, hydrocarbons, CO_2 and H_2O in the primary combustion zone. The hot char bed above the primary combustion zone reduces some of the CO_2 and H_2O produced in the primary combustion zone back to CO and H_2 (Quaak et al., 1999). A secondary air source, which is preheated by the walls of the combustion chamber, is then mixed with the combustible gases exiting the char zone to form the secondary combustion zone (Reed and Larson, 1996). Burning the combustible gases in a location that is separate from the solid fuel bed enables better mixing of the gases with air and, consequently, more complete combustion (Anderson and Reed, 2007). Primary and secondary airflow can be driven externally (e.g. by a fan or blower) or buoyantly via natural convection. A stove in which airflow is driven externally is referred to as a "forced-air" cookstove and a stove in which airflow is driven buoyantly is referred to as a "natural-draft" cookstove.

Forced-air semi-gasifier cookstoves have been shown to reduce CO and PM emissions by 90% relative to a three-stone fire in laboratory

* Corresponding author. Tel.: +1 970 491 4796.
E-mail address: marchese@colostate.edu (A.J. Marchese).

http://dx.doi.org/10.1016/j.esd.2014.07.009
0973-0826/

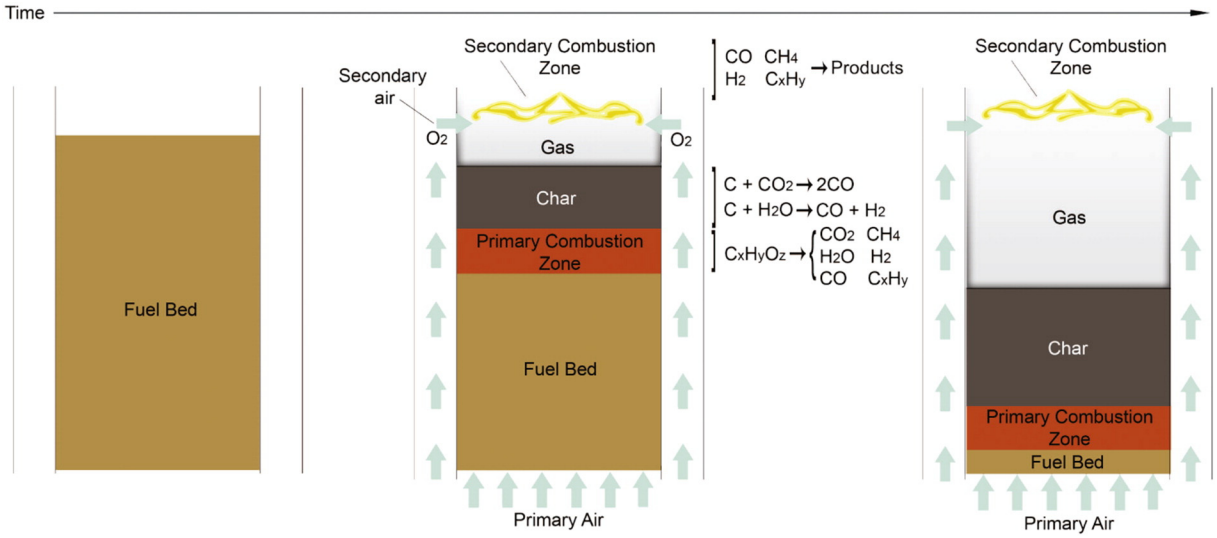

Fig. 1. Schematic of top-lit up-draft (TLUD) semi-gasifier cookstove operation.

studies (Jetter and Kariher, 2009; Jetter et al., 2012; MacCarty et al., 2010). However, the performance of semi-gasifier cookstoves has been shown to be highly variable (Jetter et al., 2012). In addition, previous work has suggested that natural-draft semi-gasifier cookstoves typically do not perform as well as forced-air semi-gasifier cookstoves (Kar et al., 2012; MacCarty et al., 2010). The objective of this study was to identify some of the underlying causes behind this observed variability. To accomplish this objective, five different configurations of natural-draft TLUD semi-gasifier household cookstoves were tested using two different fuels to determine how changes in stove design, fuel type, and operating procedure affected performance in terms of efficiency, carbon monoxide (CO) emissions, and particulate matter (PM_{10}) emissions. It was hypothesized that, although all of the cookstove configurations tested were natural-draft TLUD semi-gasifier designs that operated using the process illustrated in Fig. 1, relatively small differences in stove design would affect performance substantially. It was also hypothesized that, although semi-gasifier cookstoves have been promoted as being capable of utilizing a wide variety of fuels (Anderson and Reed, 2007), stove performance would also vary substantially with fuel type (e.g. agricultural residue versus prepared pellet fuel, as discussed by Mukunda et al. (2010)).

Methods

The matrix of cookstoves and fuel types tested, the protocol used to complete the tests, the methods used to measure carbon monoxide emissions, particulate matter emissions, fuel use, and stove temperatures, as well as the equations used to calculate efficiency, are described below. An energy balance model, which was developed using the temperature data to determine the sources of energy loss that contribute to sub-unity efficiency, is also presented below.

Test matrix

Five configurations of natural-draft TLUD semi-gasifier cookstoves were tested (see Fig. 2). The first three configurations were based on a natural-draft semi-gasifier cookstove manufactured by the Shanxi Jinqilin Energy Technology Co. Ltd. (Shanxi, China). The first configuration was this stove in its original form as received from the manufacturer ("Stove 1"). The stove was large and equipped with a chimney. The stove body was 64 cm in height, weighed 37 kg, and was constructed primarily from steel sheet metal of various thicknesses. A refractory material lined the inside of the combustion chamber and the area under the pot. The second configuration ("Stove 2") was a modified version of Stove 1, in which a cylindrical sheet metal duct was added above the secondary combustion zone to direct the flow of hot gases closer to the bottom of the pot. The third configuration ("Stove 3") was a modified version of Stove 2, in which a pot skirt was added and the chimney inlet was moved from the area under the pot to the side of the pot skirt to force the hot gases to flow around the sides of the pot. These two modified configurations were created to further investigate stove performance for the purposes of the study.

The fourth stove was the Philips HD4008. The Philips stove was smaller and had no chimney. This stove was 30 cm in height, weighed 3.6 kg, and was constructed of various steel alloys. The fifth stove was of the open-source Peko Pe design (Wendelbo, 2012). The Peko Pe stove was also a small stove without a chimney. This stove was approximately 25 cm in height, weighed 2.7 kg, and was constructed using 23 gauge stainless steel sheet metal. For simplicity, the design configurations will be referred to as Stove 1, Stove 2, Stove 3, Stove 4, and Stove 5.

The combustion chamber in each stove was cylindrical with openings at the base where primary air entered the fuel bed and openings at the top where secondary air mixed with the gases leaving the fuel bed. The fuel bed filled the combustion chamber up to the height of the secondary air inlet and the flame that heated the cooking pot was formed at the top. In most of the configurations, the secondary air entered through a ring of small holes around the circumference of the top of the combustion chamber. More information on combustion chamber geometry can be found in Section S1.1 of the Supplemental information.

The stoves were tested with two different fuel types: corn (*Zea mays*) cobs obtained from a local farm in Windsor, CO and wood pellets made from Lodgepole pine (*Pinus contorta*) by the Rocky Mountain Pellet Company (Walden, CO, USA). Corn cobs were the manufacturer-specified fuel for Stove 1. Corn cobs were collected manually off of the field after the corn had been harvested with a combine. The corn cobs were brought back to the laboratory and left to air dry for one week. Wood pellets were purchased from a local retailer in Fort Collins, CO that sells supplies for pellet stoves. The wood pellets were packaged in plastic bags and each bag of pellets weighed 18 kg.

The properties of the two fuel types are shown in Table 1. Properties with a note were obtained from the literature and properties without a note were measured. The lower heating value (LHV) of each fuel was determined by first measuring the higher heating value (HHV) using an IKA C200 Calorimeter System (IKA, Staufen, Germany). The LHV was then calculated using an estimated chemical composition for each

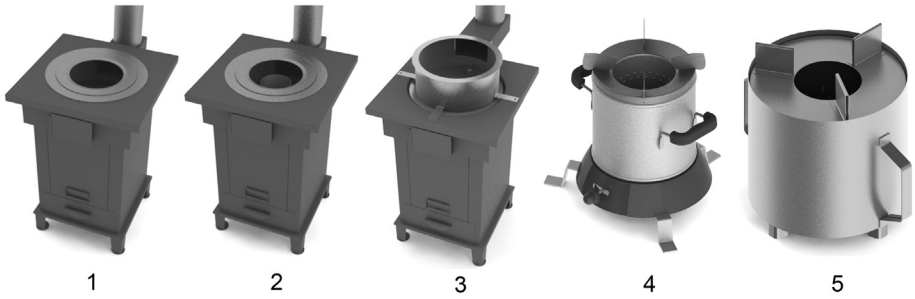

Fig. 2. Renderings of the five stoves tested. Stove 1 (Jinqilin natural-draft) was 64 cm in height, weighed 37 kg and was equipped with a chimney. Stoves 2 and 3 were modified versions of Stove 1. Stove 4 (Philips HD4008) was 30 cm in height and weighed 3.6 kg. Stove 5 (Peko Pe) was 25 cm in height and weighed 2.7 kg. Stoves 4 and 5 were not equipped with chimneys.

fuel obtained from the literature. The HHV of the char produced by each fuel type was also measured. The HHV of the char was used in place of the LHV of the char in all calculations because the chemical composition of the char was unknown.

Table 2 contains a list of all the design configuration/fuel type combinations tested. The number of replicates completed for each test is also shown. All tests were conducted by the first author.

Test protocol

The Emissions and Performance Test Protocol (EPTP), which is a modified version of the water boiling test (WBT), was used in all experiments (DeFoort et al., 2010). The WBT (The Water Boiling Test: Version 4.2.3, 2014) is the most common test used to evaluate cookstove performance in the laboratory (Chiang and Farr, 2014) and has been used in many studies on cookstove performance (Carter et al., 2014; Jetter and Kariher, 2009; Jetter et al., 2012; MacCarty et al., 2010). The EPTP was created to reduce variability between test replicates without altering the general results of the WBT (L'Orange et al., 2012). In the present study, only the cold start phase of the EPTP, in which 5 L of water is brought from 15 °C to 90 °C with the stove body starting out at room temperature, was employed. All tests were conducted in Fort Collins, CO, at an elevation of 1519 m, where water boils at 95 °C.

The corn cobs had a low bulk energy density compared to the wood pellets. This difference necessitated changes in operating procedure between tests. When the wood pellets were used, the fuel chamber of the cookstove was filled with enough wood pellets to complete the cold start test. When the corn cob fuel was used, the fuel chamber was filled completely with corn cobs. If the entire fuel bed was consumed prior to the completion of the cold start test, the stove was refueled by adding a new bed of corn cobs on top of the hot char bed while the stove was in operation. The operating procedure was varied between tests in this manner because a real-world user would be expected to refuel the stove to complete the cooking task that had been started. Indeed, Stove 1 had been designed by the manufacturer with a mechanism to enable refueling without removal of the pot.

Testing equipment

Tests were conducted in a fume hood with a 1.2 m × 1.2 m cross-section and a height of 4.3 m. The air flow rate through the hood was 0.1 $m^3\ s^{-1}$. The cross sectional area of the hood and the air flow rate were designed such that they do not affect the airflow through the stove (L'Orange et al., 2012). High efficiency particle air (HEPA) filters installed on the air inlet locations at the base of the hood prevented particulate matter in the ambient air from entering the hood. Exhaust gases were transported from the top of the hood to emission analyzers by a 12.7 cm diameter pipe.

Total mass emissions of particulate matter with an aerodynamic diameter of less than 10 μm (PM_{10}) were measured gravimetrically as described by L'Orange et al. (2012)Together, the coarse (PM_{10}–$PM_{2.5}$) and fine (<$PM_{2.5}$) PM fractions were collected on Teflon filters that were pre- and post-weighed on a Mettler Toledo MX5 microbalance (Mettler-Toledo, LLC, Columbus, OH, USA). The limit of detection (LOD) and limit of quantification (LOQ) for these measurements were 16 μg and 55 μg. All PM_{10} mass emission measurements were found to be above the LOQ with the exception of one measurement of 53 μg.

CO emissions were measured at 1 Hz with Testo 335 and Testo 350 flue gas analyzers (Testo, Sparta, NJ, USA). These analyzers used electrochemical sensors to measure the mole fraction of CO in the fume hood exhaust gas. This real-time measurement of emissions allowed the effects of changes in operating procedure on emissions to be observed. The steps that were taken to ensure that the Testo gas analyzers were measuring CO emissions accurately are described in Section S1.2 of the Supplemental Information.

Real-time temperature data were acquired at 1 Hz from 17 to 24 type K thermocouples (Omega Engineering, Stamford, CT, USA) installed on each stove. Gas temperature measurements included inlet air temperature, preheated secondary air temperature, and exhaust gas temperature. Temperatures were also recorded at various locations in the fuel chamber and on the outside of the stove body. An additional type K thermocouple submerged in the pot of water measured the water temperature at 0.6875 Hz. A program, created in LabVIEW™, monitored the water temperature, controlled the airflow rate through

Table 1
Properties of the corn cob and wood pellet fuels.

Fuel type	Bulk density ($kg\ m^{-3}$)	Density ($kg\ m^{-3}$)	LHV_{daf} ($J\ g^{-1}$)	Moisture content (mass fraction)	Ash content (mass fraction)
Corn cobs	195[a]	340[b]	18,119	8.1% ± 0.1%	<2%
Wood pellets	696[c]	1260 ± 55	19,560	5.5% ± 0.6%	<1%

[a] Coovattanachai (1989).
[b] Lin et al. (1995).
[c] Rocky Mountain Pellet Company, Inc. (2012).

Table 2
Table of tests conducted.

Configuration	Fuel type	No. of replicates
Stove 1 (Jinqilin natural-draft)	Corn cobs	4
Stove 1 (Jinqilin natural-draft)	Wood pellets	3
Stove 2	Corn cobs	2
Stove 2	Wood pellets	3
Stove 3	Corn cobs	3
Stove 3	Wood pellets	3
Stove 4 (Philips HD4008)	Corn cobs	3
Stove 4 (Philips HD4008)	Wood pellets	3
Stove 5 (Peko Pe)	Corn cobs	3
Stove 5 (Peko Pe)	Wood pellets	3

the fume hood, and recorded the starting and ending time for each test. More information on the instrumentation used for data collection can be found in Section S1.2 of the Supplemental Information.

Efficiency calculations

In addition to the emissions and temperature measurements described above, fuel consumption measurements were made for each of the configuration/fuel type combinations in Table 2. The equations that were used to calculate efficiency based on these measurements are described below.

The *thermal efficiency* of each stove is defined as the ratio of the energy transferred to the water to the difference between the energy available in the fuel and the energy contained in the char remaining at the end of the test. Thermal efficiency is calculated using Eq. (1) (DeFoort et al., 2010):

$$\eta = \frac{c_{p,H2O} m_{H2O} \Delta T_{H2O} + h_{v,H2O} m_{H2Oevap}}{m_f \left(1 - MC_f\right) LHV_{f,dry} - m_f MC_f \left(c_{p,H2O} \Delta T_{H2O,f} + h_{v,H2O}\right) - LHV_c m_c} \quad (1)$$

where $c_{p,H2O}$ is the specific heat of water (J g^{-1} K^{-1}), m_{H2O} is the mass of water boiled (g), ΔT_{H2O} is the change in the water temperature between the beginning and end of the test (K), $h_{v,H2O}$ is the heat of vaporization of water (J g^{-1}), $m_{H2Oevap}$ is the mass of water evaporated out of the pot during the test (g), m_f is the mass of wet fuel consumed (g), MC_f is the moisture content of the fuel (as a mass fraction on a wet basis), $LHV_{f,dry}$ is the lower heating value of the fuel on a dry basis (J g^{-1}), $\Delta T_{H2O,f}$ is the temperature change that the water in the fuel had to undergo before it was evaporated (assumed to be 75 K), LHV_c is the lower heating value of the charcoal produced from the fuel (J g^{-1}), and m_c is the mass of the ash and charcoal remaining at the end of the test (g).

The *overall efficiency* of each stove is defined herein as the ratio of the energy transferred to the water to the energy available in the dry mass of fuel consumed (Eq. (2)).

$$\eta_{OA} = \frac{c_{p,H2O} m_{H2O} \Delta T_{H2O} + h_{v,H2O} m_{H2Oevap}}{m_f \left(1 - MC_f\right) LHV_{f,dry} - m_f MC_f \left(c_{p,H2O} \Delta T_{H2O,f} + h_{v,H2O}\right)} \quad (2)$$

In this formulation, the energy remaining in the charcoal left at the end of the test represents an energy loss. Although the chemical energy contained in this char is still available for subsequent use, it should not be assumed that it will be converted into thermal energy (Kar et al., 2012). It should be noted, however, that most studies on stove performance do account for the energy remaining in the char and report the thermal efficiency shown in Eq. (1) (Jetter and Kariher, 2009; Jetter et al., 2012; MacCarty et al., 2010).

Energy balance model

To determine the major sources of efficiency loss and to inform future design efforts, all of the energy sources, sinks, and components of energy transfer present during stove operation were accounted for in a thermodynamic energy balance model. The sources of energy include the energy in the fuel and the energy in the inlet air. The energy contained in the char remaining at the end of the test was counted as an energy sink. The energy transfer components included the energy transferred to the water, the energy transferred to (and stored in) the stove body, the energy lost through convection and radiation heat transfer from the outside of the stove body to the surroundings, and the energy lost through the exhaust gases.

The portion of the energy contained in the fuel that could have been used to heat the cooking surface was calculated using Eq. (3):

$$E_f = m_f \left(1 - MC_f\right) LHV_{f,dry} - m_f MC_f \left(c_{p,H2O} \Delta T_{H2O,f} + h_{v,H2O}\right) \quad (3)$$

where m_f is the mass of fuel consumed (g), MC_f is the moisture content of the fuel (as a mass fraction on a wet basis), $LHV_{f,dry}$ is the lower heating value of the dry fuel (J g^{-1}), $\Delta T_{H2O,f}$ is the temperature change that the water in the fuel had to undergo before it was evaporated (assumed to be 75 K), and $h_{v,H2O}$ is the heat of vaporization of water (J g^{-1}). The second term on the right hand side of Eq. (3) represents energy contained in the fuel that had to be used to evaporate the water stored in the fuel.

The energy transferred to the water was calculated using Eq. (4):

$$E_{H2O} = m_{H2O} c_{p,H2O} \left(T_f - T_i\right) + h_{v,H2O} m_{H2Oevap} \quad (4)$$

where E_{H2O} is the energy transferred to the water (J), m_{H2O} is the mass of water (kg), $c_{p,H2O}$ is the specific heat of the water (J kg^{-1} K^{-1}), T_f is the final temperature of the water (90 °C), T_i is the initial temperature of the water (13 °C to 17 °C), $h_{v,H2O}$ is the heat of vaporization of water (2260 J g^{-1}), and $m_{H2Oevap}$ is the mass of water evaporated out of the pot during the test (g).

The energy contained in the char remaining at the end of the test was calculated using Eq. (5):

$$E_c = m_c HHV_c \quad (5)$$

where E_c is the energy contained in the char (J), m_c is the mass of char (g), and HHV_c is the higher heating value of the char (J g^{-1}).

For Stoves 4 and 5, the energy added to the stove body was calculated by multiplying the mass of the stove by the specific heat of the metallic stove body and the change in temperature of the stove body between the beginning and end of the test (Eq. (6)).

$$E_{stove} = m_{stove} C \left(T_f - T_i\right) \quad (6)$$

where E_{stove} is the energy stored in the stove body (J), m_{stove} is the mass of the stove (kg), C is the specific heat of the material the stove is constructed from (J kg^{-1} K^{-1}), T_f is the final temperature of the stove body (K), and T_i is the initial temperature of the stove body (K). The specific alloys from which Stoves 4 and 5 were constructed were unknown and properties of plain carbon steel and AISI 304 stainless steel were assumed for these calculations.

Calculating the quantity of the energy stored in the bodies of Stoves 1, 2, and 3 was more complicated because, although these stoves were constructed primarily of steel, the stove bodies also contained a large mass of dense refractory material. The refractory material was expected to be at a higher temperature than the steel frame because the refractory material was directly exposed to the hot gases that passed under the pot. The large mass and low thermal conductivity of the refractory material (in comparison to the steel) required the development of an additional heat transfer model to determine the quantity of thermal energy stored in the refractory material. More information on this heat transfer model can be found in the Section S2 of the Supplemental Information.

The energy stored in the steel frame was calculated by multiplying the mass of the frame by the specific heat of the frame and the change in temperature between the beginning and end of the test:

$$E_{frame} = m_{steel} C_{steel} \left(T_f - T_i\right) \quad (7)$$

where E_{frame} is the energy stored in the steel frame (J), m_{steel} is the mass of the steel frame (25 kg), C_{steel} is the specific heat of the specific heat of plain carbon steel (434 J kg^{-1} K^{-1}) (Incropera et al., 2007), T_f is the

temperature of the steel frame at the end of the test (K), and T_i is the temperature of the steel frame at the beginning of the test (K). At each time step the entire steel frame was assumed to be at the average temperature measured by the four thermocouples installed on the outside walls of the stove.

For Stoves 1, 2, and 3, the total energy stored in the stove body was calculated by adding the amount of energy stored in the steel frame to the amount of energy stored in the block of refractory material:

$$E_{stove\ body} = E_{frame} + E_{block}. \tag{8}$$

The heat lost through convection from the stove body was calculated using Eq. (9):

$$E_{conv} = \int_0^{t_f} h(t)A[T(t) - T_\infty]dt \tag{9}$$

where E_{conv} is the energy lost through convection (J), h is the convection coefficient ($Wm^{-2}\ K^{-1}$), A is the surface area of the sides of the stove (m^2), T is the temperature of the stove body (K), T_∞ is the temperature of the surroundings (K), and t_f is the length of the test (s).

Eq. (9) was integrated numerically using the outside stove body temperature that was recorded every second during the test as $T(t)$. The Rayleigh number, Nusselt number, and the convection coefficient were recalculated at every time step. The average of the primary and secondary air inlet temperatures at time 0 was taken as the ambient air temperature.

The outer surfaces of Stoves 1, 2, and 3 were modeled as 4 vertical plates. The outer surfaces of Stoves 4 and 5 were modeled as single vertical plates with surface areas equal to the surface areas of the cylindrical outer walls. The outside walls were assumed to be isothermal at each time step. The convection coefficient was calculated using the Nusselt number correlation for natural convection over a vertical flat plate shown in Eq. (10) (Churchill and Chu, 1975).

$$\overline{Nu}_L = 0.68 + \frac{0.670{Ra_L}^{1/4}}{\left[1 + (0.492/Pr)^{9/16}\right]^{4/9}}, \quad Ra_L \le 10^9 \tag{10}$$

where $\overline{Nu}_L$ is the average Nusselt number over the length of the plate, Ra_L is the Rayleigh number, and Pr is the Prandtl number (0.7 for air).

The convection coefficient was calculated from the Nusselt number as shown in Eq. (11) (Incropera et al., 2007):

$$\overline{h}_L = \frac{\overline{Nu}_L\ k}{L} \tag{11}$$

where k is the thermal conductivity of the air ($W\ m^{-1}\ K^{-1}$).

The radiation heat loss from the stove body was calculated using Eq. (12):

$$E_{rad} = \int_0^{t_f} \epsilon\sigma A\left[T(t)^4 - {T_\infty}^4\right]\ dt \tag{12}$$

where E_{rad} is the energy lost through radiation (J), ϵ is the emissivity of the stove, σ is the Stefan–Boltzmann constant ($W\ m^{-2}\ K^{-4}$), A is the surface area of the stove (m^2), $T(t)$ is the temperature of the stove body (K), and T_∞ is the temperature of the surroundings (K). Eq. (12) was integrated numerically using the same temperatures used in Eq. (9).

The amount of energy transferred to the water, contained in the char at the end of the test, stored in the stove body, and lost through radiation and convection from the outside walls of the stove was subtracted from the total energy contained in the fuel input at the beginning of the test. The difference was taken to be the amount of energy lost through the exhaust from the stove.

Results and discussion

The high power carbon monoxide emissions, high power particulate matter emissions, and thermal efficiencies measured during the experiments, as well as the results of the energy balance calculations, are presented below. First, the differences between the results for each design configuration/fuel type combination are presented. Second, the results are compared to the tier ratings for biomass cookstove performance established at the ISO International Workshop on Clean and Efficient Cookstoves. Third, the real-time carbon monoxide emission measurements are used to identify large, transient increases in emissions associated with refueling of semi-gasifier cookstoves. Fourth, some further discussion on the emissions results is provided. Fifth, the results of the energy balance model are presented.

Influence of design configuration and fuel type on emissions and efficiency

As shown in Fig. 3, the high-power CO and PM_{10} emissions from all five configurations varied substantially with fuel type. In general, the measured emissions were lower when wood pellets were used as fuel instead of corn cobs. For example, when Stove 1 was fueled with wood pellets instead of corn cobs, CO emissions decreased by a factor of 47 and PM_{10} emissions decreased by a factor of 6. Similarly, when Stove 4 stove was fueled with wood pellets instead of corn cobs, CO emissions decreased by a factor of 2. When Stove 5 was fueled with wood pellets instead of corn cobs, CO emissions decreased by a factor of 11 and PM_{10} emissions decreased by a factor of 3.

Although the design changes made to Stove 1 resulted in reduced emissions, Stoves 1, 2, and 3 generally produced much higher emissions than both Stoves 4 and 5. Stove 5 exhibited the lowest emissions overall. As shown in Fig. 4, Stoves 4 and 5 were also more efficient than Stoves 1, 2, and 3.

Unlike emissions, thermal efficiency was not affected by fuel type (Fig. 4). The average thermal efficiencies for Stove 1 fueled with corn cobs and Stove 1 fueled with wood pellets were 8.3% and 9.0%, respectively. The average thermal efficiencies for Stove 2 fueled with corn cobs and Stove 2 fueled with wood pellets were 12.3% and 12.2%. Similarly, the average thermal efficiencies for Stove 3 fueled with corn cobs and Stove 3 fueled with wood pellets were 20.1% and 19.9%. The thermal efficiency of a given design configuration is expected to depend primarily upon stove geometry.

Comparison to tiers for cookstove performance

In Figs. 3 and 4, the performance of each stove has been compared to the tier ratings for high-power CO emissions, high-power PM emissions, and high-power efficiency established at the ISO International Workshop on Clean and Efficient Cookstoves. For each parameter, 5 levels of performance ranging from Tier 0 to Tier 4 are included (ISO International Workshop on Clean and Efficient Cookstoves, 2012). Tier 0 represents a stove that is comparable to or worse than a three stone fire or traditional stove. Tier 4 represents a highly performing stove that would be expected to decrease health risks substantially if it were to completely replace the traditional stove. Tiers 1 through 3 represent various levels of improved stoves.

In terms of these tier ratings, Stoves 1, 2, and 3 had the most variable performance, which ranged from Tier 0 to Tier 3 depending on the fuel type and design configuration implemented. The performance of Stove 4 was the least variable; emissions remained within Tier 2 for both fuel types. Emissions from Stove 5 were on the border between Tier 2 and Tier 3 when the stove was fueled with corn cobs and on the border between Tier 3 and Tier 4 when the stove was fueled with wood pellets (Fig. 3). Although several of the configuration/fuel type combinations met the Tier 4 high-power CO rating, only Stove 5 operating on wood pellets came close to meeting the Tier 4 high-power PM rating. The emission results for Stove 5 are noteworthy since previous studies

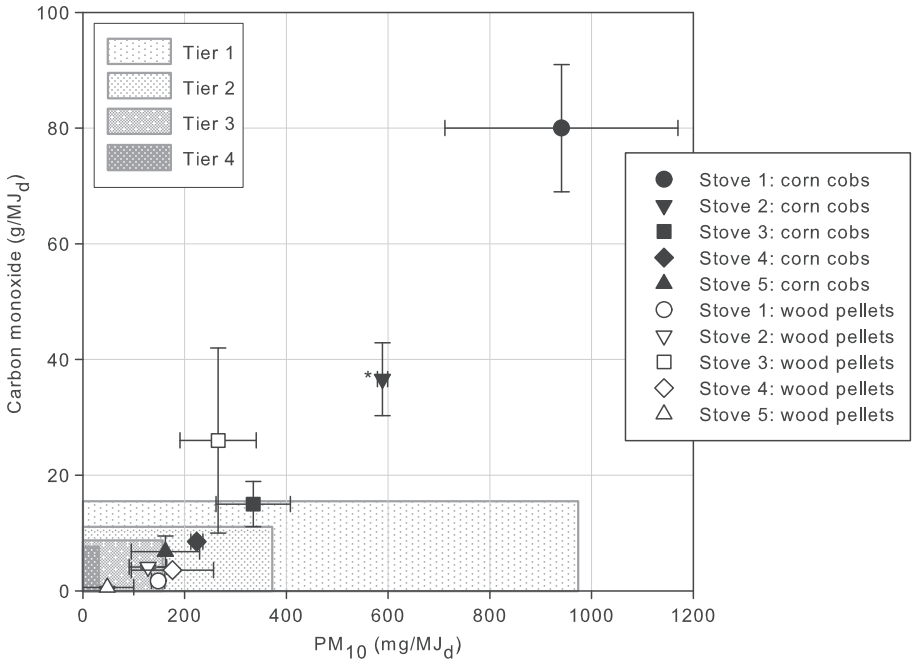

Fig. 3. High power carbon monoxide emissions vs. high power particulate matter emissions compared to ISO tiers for biomass stove performance. Error bars represent one standard deviation with the exception of the error bars on the data point for Stove 2 fueled with corn cobs. This data point (marked with an asterisk) is based on only two test replicates and the error bars represent the total range of the two results.

suggested that such low particulate matter emissions were only achievable with forced-air semi-gasifier cookstoves (Jetter et al., 2012). These results suggest that natural-draft TLUD semi-gasifier cookstoves have the potential to meet both of the high power Tier 4 emission ratings.

Emission increases associated with refueling

The two design changes made to Stove 1 to create Stoves 2 and 3 were motivated by the low efficiencies measured with Stove 1. The efficiency increased when the cylindrical duct and pot skirt were added above the secondary combustion zone. The effect of these design changes on CO and PM_{10} emissions varied depending on the fuel type. Specifically, when corn cobs were used as a fuel, emissions from Stoves 2 and 3 were lower than those from Stove 1. When wood pellets were used as a fuel, emissions from Stoves 2 and 3 were higher than those from Stove 1 (Fig. 4).

The high CO emissions observed when Stove 1 was operated using corn cob fuel resulted from the need to refuel the stove prior to completion of the cold start test due to the low bulk energy content in the corn cobs and high thermal mass of the stove. This determination was made

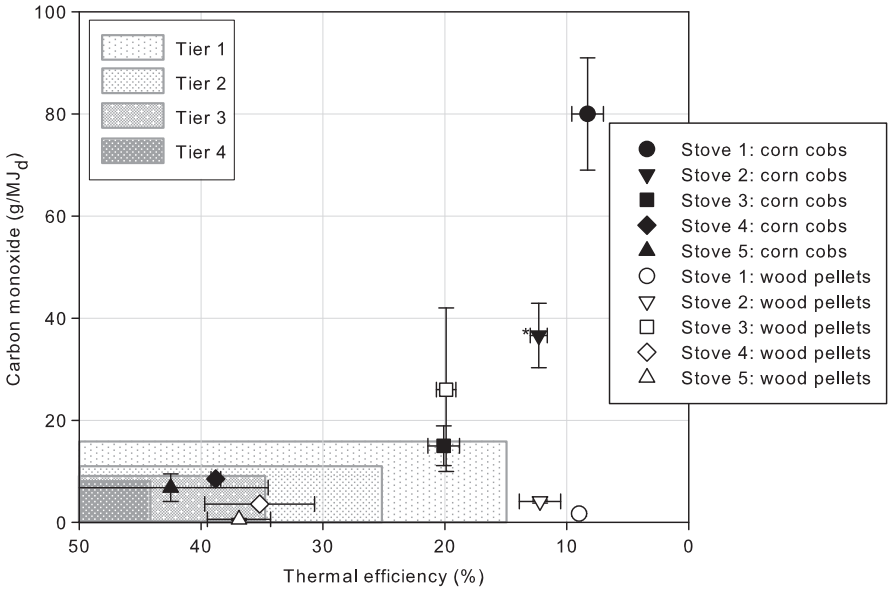

Fig. 4. High power carbon monoxide emissions vs. thermal efficiency compared to ISO tiers for biomass stove performance. Error bars represent one standard deviation with the exception of the error bars on the data point for Stove 2 fueled with corn cobs. This data point (marked with an asterisk) is based on only two test replicates and the error bars represent the total range of the two results.

by comparing real-time CO measurements with real-time temperature measurements taken inside the fuel chamber. Fuel bed temperature measurements allowed tracking of the primary combustion zone during stove operation. Data from a representative cold start performed with Stove 1 and corn cob fuel are shown in Fig. 5a. CO emission levels were lowest at the beginning of the test, just after ignition, when gasification had not yet started. CO emissions became noticeably higher once gasification started. Emissions increased once again when the entire fuel bed had gasified and the char began to burn. After the char was burnt, fuel had to be added to continue the test. Subsequent batches of fuel were consumed quickly and carbon monoxide emissions became higher than at any other point during the test. During these times the stove was no longer operating purely as a TLUD semi-gasifier. Refueling may have also resulted in sharp increases in PM emissions, but real-time PM emissions were not measured in this study.

Similar CO emission trends were observed when Stoves 2 and 3 were operated using corn cob fuel. The modifications to Stove 1 did not reduce CO emission levels for the first batch of fuel substantially. However, because Stoves 2 and 3 exhibited improved the heat transfer to the pot, the stoves were refueled fewer times. The lower overall emissions for the tests were the result of reducing the number of emission spikes. For Stove 2, consumption of the original batch of corn cob fuel proceeded more slowly than in Stove 1 and the stove only had to be refueled once during the test (Fig. 5c). For Stove 3, the approximate time to boil was reduced from 25 min (for Stove 1) to 15 min and the stove did not have to be refueled during the test (Fig. 5e).

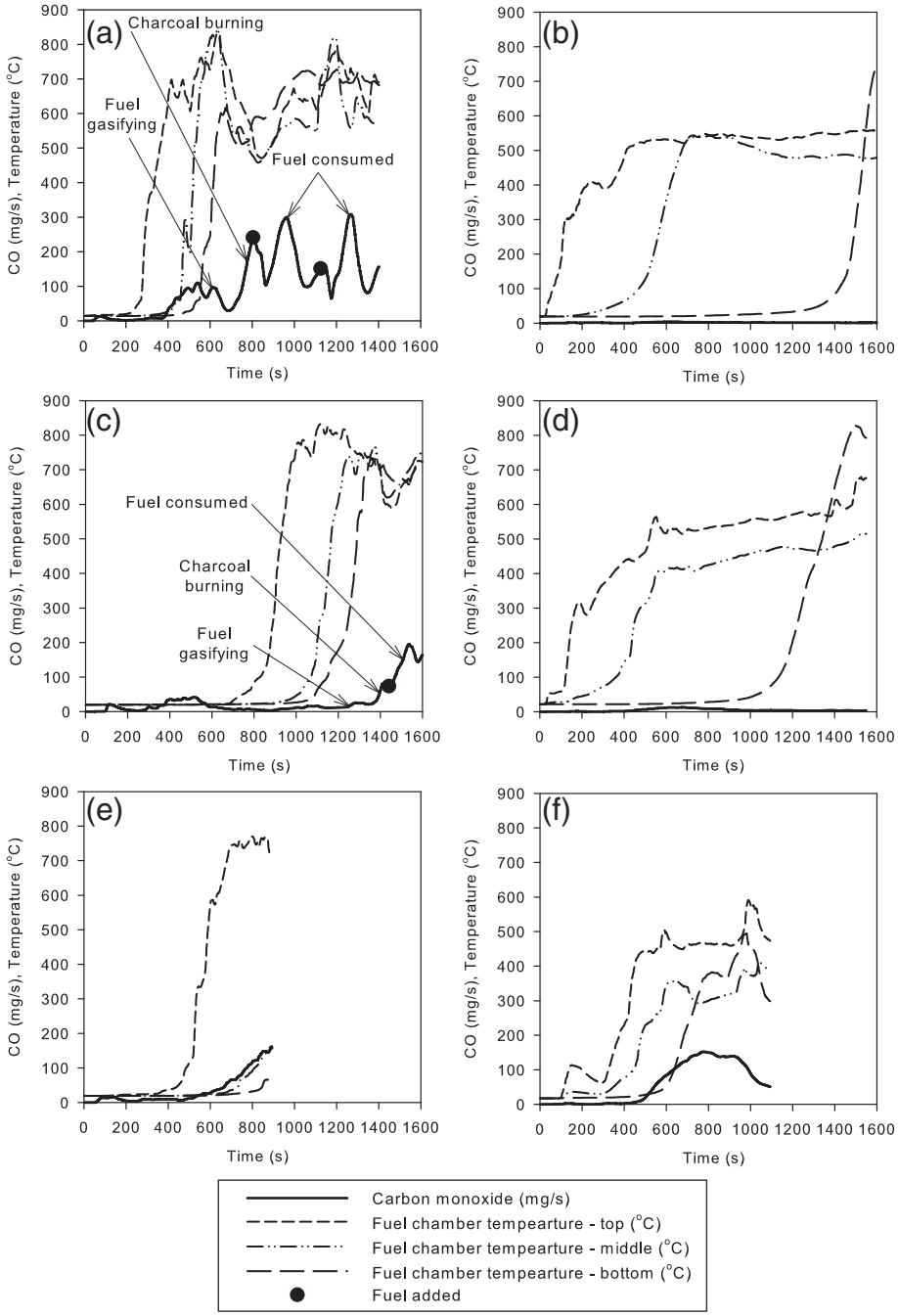

Fig. 5. CO emissions and fuel chamber temperatures during a cold start test done with (a) Stove 1 and corn cob fuel, (b) Stove 1 and wood pellet fuel, (c) Stove 2 and corn cob fuel, (d) Stove 2 and wood pellet fuel, (e) Stove 3 and corn cob fuel, and (f) Stove 3 and wood pellet fuel.

When Stove 1 was fueled with wood pellets, extremely low CO emissions were observed (Fig. 5b). In this case, Stove 1 did not require refueling prior to completion of the test. Emissions from Stove 2 were not substantially different (see Fig. 5b and d). However, emission levels from Stove 3 were higher (Fig. 5f). In this configuration, the modifications may have affected the airflow through the stove and enhanced heat transfer from the hot gases to the pot may have actually limited the oxidation of pollutants by reducing the gas temperature.

The performance of Stove 4 did not vary as substantially with fuel type in comparison to Stoves 1, 2, and 3. As shown in Fig. 6, the CO emissions were slightly higher for Stove 4 when the corn cob fuel was used. Stove 4 had to be refueled once during the cold start when corn cobs were used. However, a dramatic increase in emission rate was not observed upon refueling. Stove 5 did not require refueling during the cold start when either fuel was used (Fig. 7).

These results illustrate how the bulk energy density of the fuel impacts the CO emissions. It is understood that the choice of fuel type used in the field is dictated by cost and availability. However, the results underscore the need to incorporate the fuel type that the consumer is known to be most likely to use into the stove design for TLUD semi-gasifier cookstoves.

These results also illustrate how changes in operator behavior can have a large affect on stove performance. This point has been illustrated with other types of cookstoves in previous studies. Jetter et al. (2012) tested a three stone fire and two rocket elbow stoves under different operating conditions and observed a substantial variation in emissions performance. If the natural-draft TLUD semi-gasifier cookstoves tested in this study were to be tested by different operators, either in the laboratory or under real-world conditions, the technique used by different operators to refuel the stove, and the frequency at which different operators refueled, would most likely lead to substantial variability in the results. Since refueling has been demonstrated to result in large, transient increases in CO emission rate, semi-gasifier cookstove dissemination projects should be accompanied by training to educate users on the issues associated with adding fuel onto the hot char bed.

Further discussion on the experimental results

Because only the cold start phase of the EPTP was completed, the results do not provide a complete picture of the performance of each stove. The results of the hot start phase are also typically considered when evaluating high-power performance, and ISO IWA tiers were also established for low-power emissions and fuel consumption (ISO International Workshopon Clean and Efficient Cookstoves, 2012). However, the purpose of this study was not to provide a comprehensive review of stove performance. Rather, the purpose was to illustrate how performance could vary between five different stove configurations that operate under the same natural-draft TLUD semi-gasifier operating principle.

Another limitation associated with the experimental results is the small sample sizes used and the high variance associated with the CO and PM_{10} measurements. This variance is illustrated by the error bars, which depict one standard deviation, in Figs. 3 and 4. The use of larger sample sizes would have improved the level of confidence in the overall magnitudes of the emission measurements. However, the experimental results illustrate the range of performance that is possible with natural-draft TLUD semi-gasifier cookstoves, and the real-time carbon monoxide emission measurements illustrate how strongly performance can be affected by fuel type, operating conditions, and user behavior. Efficiency measurements, on the other hand, were less variable and the coefficient of variance for all efficiency measurements was below 20%.

Three of the design configurations tested (Stoves 1, 2, and 3) included chimneys. In addition to the tiers for overall high-power emissions, ISO IWA tiers for indoor emissions have been established (ISO International Workshopon Clean and Efficient Cookstoves, 2012) to help evaluate the potential for improving user health by using a chimney to direct emissions away from the user and out of the home. Indoor emissions, which represent the difference between the total emissions from the stove and the portion of those emissions that would be directed out of the home through the chimney, were not measured in this study. Consequently, the total emissions from the chimney stoves may not necessarily be comparable to the total emissions from the non-chimney stoves from the perspective of health impacts. However, field studies involving chimney stoves have shown that not all of the emissions produced by a chimney stove are directed out of the home and that high concentrations of CO and PM may still be measured inside homes with chimney stoves (Naeher et al., 2000; Northcross et al., 2010; Tian et al., 2009). Because a portion of the emissions produced by a chimney stove are expected to remain in the home, lower overall emissions from chimney stoves are expected to correlate with lower indoor emissions.

It should also be noted that all five stoves exhibited carbon monoxide emission spikes during shut-down. These spikes are not shown in Figs. 5 through 7, however, because emissions from the shut-down

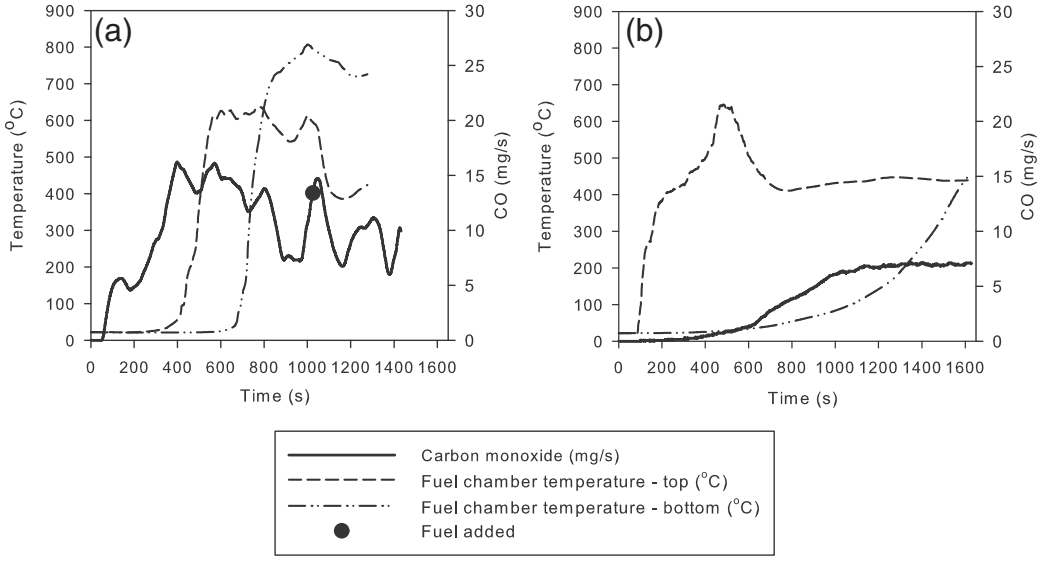

Fig. 6. CO emissions and fuel chamber temperatures during a cold start test done using Stove 4 (a) with corn cob fuel and (b) with wood pellet fuel.

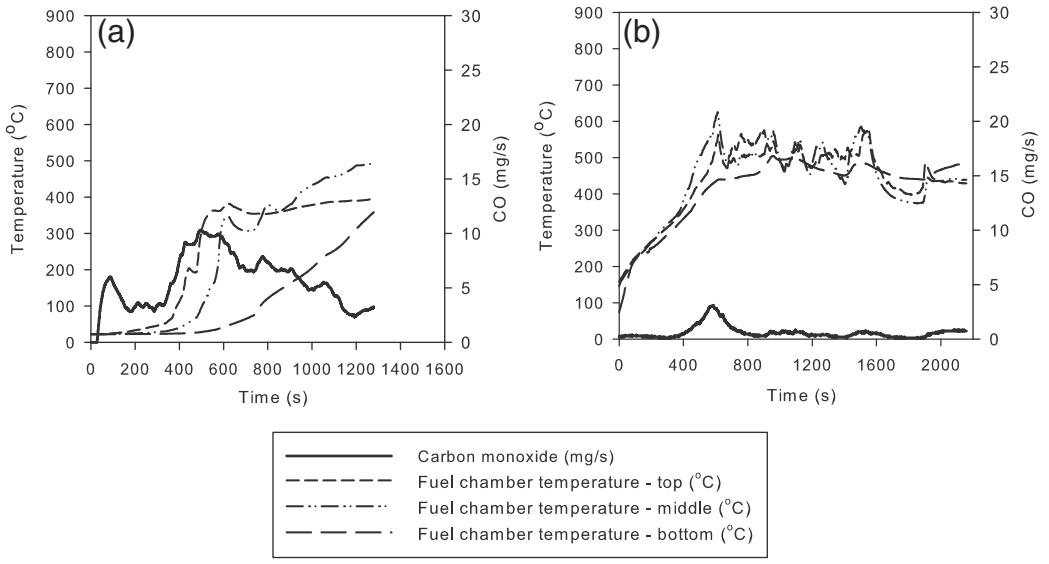

Fig. 7. CO emissions and fuel chamber temperatures during a cold start test done using Stove 5 (a) with corn cob fuel and (b) with wood pellet fuel.

process are not included in the EPTP or any other water boiling test. However, the existence of shut-down emissions, as well as mitigation methods, should be considered since users will be exposed to these emissions during real-world use of semi-gasifier cookstoves.

Energy balance results

The results of the energy balance model are shown in Figs. 8 and 9. The calculated quantities of energy transferred to the water and stove body; remaining in the char; and transferred out of the stove via the exhaust gases, convection and radiation are shown. For each configuration/fuel type combination, the results are reported in terms of total energy required to complete the cold start test (Fig. 8) and as a fraction of the total energy contained in the fuel input into the stove during the test (Fig. 9).

Stove 1 used the greatest amount of energy to complete the test (Fig. 8). Compared to Stoves 4 and 5, Stoves 1, 2 and 3 had more heat addition to the stove body and energy transferred out of the stove via the exhaust gases. These larger losses were the result of the high thermal mass of Stoves 1, 2, and 3 as well as the presence of the chimney (MacCarty et al., 2010). The thermal efficiency of a cookstove is primarily dependent upon the ability to transfer heat to the cooking surface through radiation from the flame and convection from the hot gases. The amount of heat transferred to the cooking surface by convection is proportional to the area over which the hot gases flow. Stoves 1 and 2 only allowed heat to be transferred to the pot by radiation and by hot gases impinging on the bottom of the pot. The surface area for convection was limited to the area of the bottom of the pot. Consequently, thermal efficiencies were low in these configurations. Stove 3, which included a pot skirt, had a larger area over which convective heat transfer to the pot could occur because the hot gases were forced to flow around

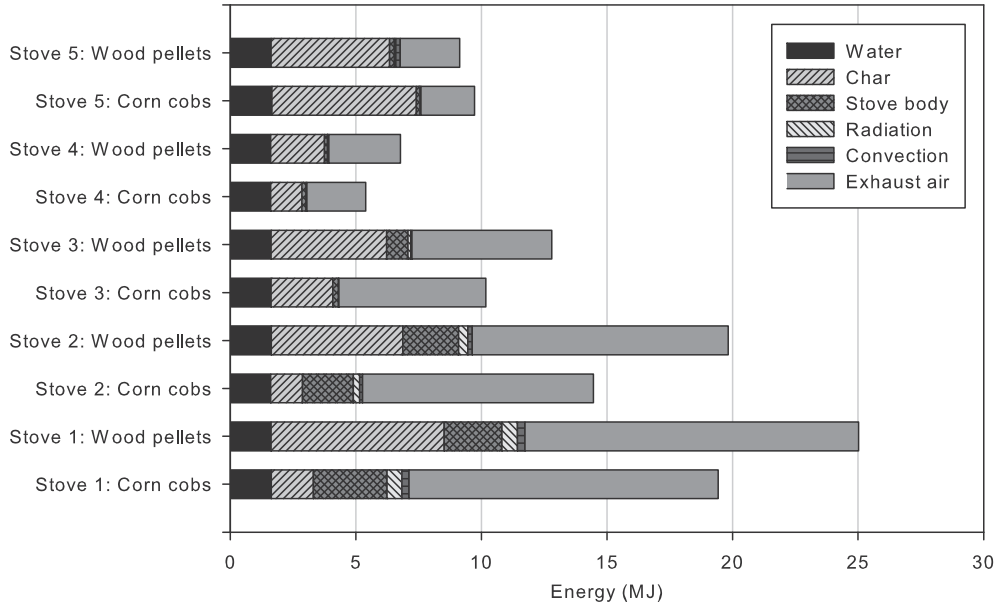

Fig. 8. Results of the energy balance with the total energy consumption attributed to each component shown. The overall length of the bar for each test case represents the total energy input into the stove, in the form of fuel, to bring 5 L of water from 15 °C to 90 °C.

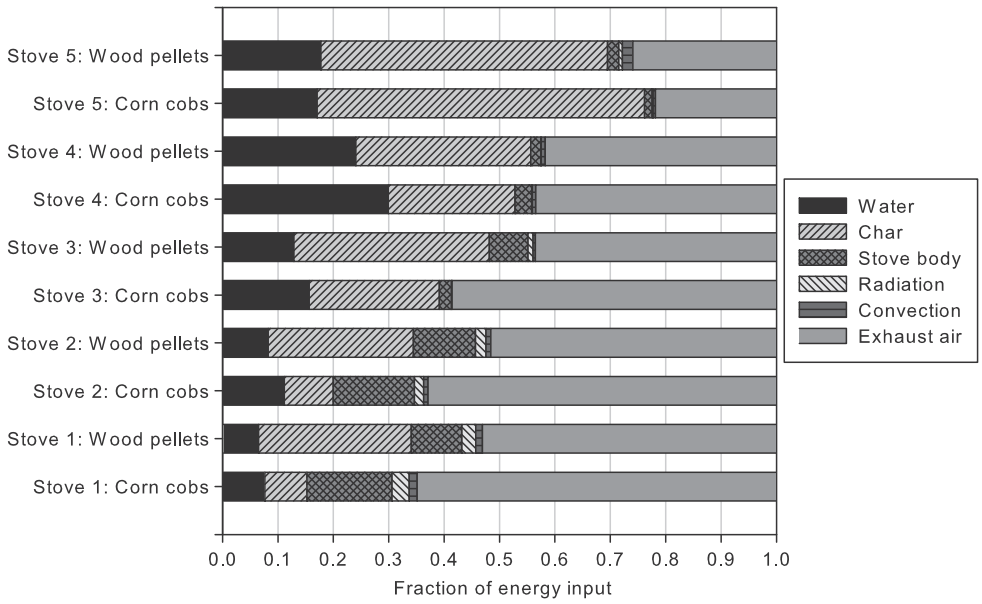

Fig. 9. Results of the energy balance with the total energy consumption attributed to each component shown as a percentage of total energy consumption.

the sides of the pot. It should be noted that, for Stove 3, a faster time to boil also resulted in reduced energy losses due to stove body heating, despite the high thermal mass of the stove, as evidenced by the results for Stoves 2 and 3 operating with corn cobs. These results suggest that the stove body never reached a steady state temperature.

For Stoves 4 and 5, which had lower thermal masses due to their smaller sizes and lack of refractory lining, energy losses due to stove body heating, convection, and radiation were all very low (Fig. 8). Although the thermal efficiencies of Stoves 4 and 5 were comparable (Fig. 4), Stove 5 used more energy to complete the test than Stove 4 (Fig. 8). This difference was due to the fact that a large amount of the energy input to Stove 5 was left over as char at the end of the test (Fig. 9).

As shown in Fig. 9, a large fraction of the energy input into a semi-gasifier cookstove in the form of fuel may be left over in the form of char at the end of the test. Most notably, an average of 52% and 59% of the energy input was left over as char at the end of the test for Stove 5 fueled with corn cobs and wood pellets, respectively. This value was 28% for Stove 1 fueled with wood pellets, 26% for Stove 2 fueled with wood pellets, 23% for Stove 3 fueled with corn cobs, 35% for Stove 3 fueled with wood pellets, 23% for Stove 4 fueled with corn cobs, and 32% for Stove 4 fueled with wood pellets. These results illustrate why it is important to consider the difference between the thermal efficiency and overall efficiency when evaluating a semi-gasifier cookstove—especially if the cookstove has been designed to produce charcoal or biochar. Although the average thermal efficiency of Stove 5 was approximately 42%, the average overall efficiency was only 17% (Fig. 9).

If the char that is left over after the fuel is gasified is put to some use (for example, as a fuel in a charcoal-burning stove or as a soil amendment), the low overall efficiency may not be a disadvantage to the stove user. For example, some combination TLUD/charcoal cookstoves have been designed in which the fuel chamber can be removed to transform a semi-gasifier cookstove into a charcoal stove once the gasification process is complete (for an example, see Wisdom Innovations (2013)). However, it is recommended that testing protocols include a calculation of efficiency, similar to the "overall efficiency" calculation used in this study and shown in Eq. (2), in which the energy remaining in the char at the end of the test is *not* subtracted from the energy input into the stove in the form of fuel. The thermal efficiency calculation typically used in the WBT and EPTP test protocols (DeFoort et al., 2010; The Water Boiling Test: Version 4.2.3, 2014) is primarily a measure of how efficiently heat is transferred to the pot and does not always reflect how efficiently a given stove uses fuel overall.

Conclusions

The results of this study illustrate that differences in stove design can lead to a wide variation in performance among different natural-draft TLUD semi-gasifier cookstoves. In addition, changes in fuel type and operating procedure can have a profound effect on the exhaust emissions for the same natural-draft TLUD semi-gasifier cookstove. The results show that natural-draft TLUD semi-gasifier cookstoves do have the potential to achieve low emissions when operated under controlled conditions (specified fuel type and operating procedure). Additional work is needed to develop a natural draft semi-gasifier cookstove that achieves Tier 4 performance, but the results of this study suggest that Tier 4 high-power emissions and thermal efficiency may be within reach using this relatively simple design.

The instantaneous CO and temperature measurements strongly suggest that refueling TLUD semi-gasifier cookstoves results in a sharp increase in CO emissions. In the field, there is no guarantee that users will refrain from refueling the stove during operation and thereby be exposed to high emissions. Improving the thermal efficiency of a stove can reduce the incidence of these transient increases in CO emissions by increasing the amount of useful energy that can be delivered to the cooking surface without refueling. However, eliminating these transient increases altogether by developing a stove design that can respond to transient conditions will be necessary to ensure low CO emissions in the field. Overall, it is important to consider real-world operating conditions when designing a semi-gasifier cookstove and efforts should not focus only on designing a stove that performs well during laboratory tests and achieves high ratings according to the ISO IWA tiers. Specifically, the effects that all modes of stove operation, including refueling, transition to char combustion, and shut-down, have on emissions should be considered even if these operational modes do not necessarily occur during the course of a WBT.

Stoves should be tested in the laboratory using as many fuels that may be used in the field as possible. Existing TLUD semi-gasifier cookstove designs should not be promoted as capable of utilizing any biomass as fuel. Although the stove will function using a wide variety of fuels, emissions performance will vary substantially. This study clearly

shows that TLUD semi-gasifier cookstoves that exhibit very low emissions with one fuel type may exhibit very high emissions with another fuel type. Accordingly, further research and development efforts must be aimed at developing cookstove designs whose emissions and performance are more robust and not as strongly affected by the solid biomass fuel type and/or stove operating conditions.

Furthermore, the results of the energy balance modeling illustrate that, for some designs, up to 60% of the energy contained in the fuel that is consumed by TLUD semi-gasifier cookstoves is left over in the form of char after the fuel bed is gasified. This result illustrates the importance of considering the difference between the fraction of the energy *released* from the fuel that is transferred to the cooking pot and the fraction of the energy contained in the total mass of fuel consumed that is transferred to the cooking pot. It is also important to consider whether or not the char that is produced will be useful to the target consumer.

Acknowledgments

The authors acknowledge the National Science Foundation for providing a graduate research fellowship to Jessica Tryner (NSF DGE 0801707) and Impact Carbon for funding a portion of the experiments. The authors also acknowledge the support of the U.S. Department of Energy award number DE-EE006086.

Appendix A. Supplementary data

Supplementary data to this article can be found online at http://dx.doi.org/10.1016/j.esd.2014.07.009.

References

Anderson PS, Reed TB. Micro-gasification: what it is and why it works. Boiling Point 2007;53:35–7.
Bonjour S, Adair-Rohani H, Wolf J, Bruce NG, Mehta S, Prüss-Ustün A, et al. Solid fuel use for household cooking: country and regional estimates for 1980–2010. Environ Health Perspect 2013;121(7):784–90. http://dx.doi.org/10.1289/ehp.1205987.
Bruce N, Rehfuess E, Mehta S, Hutton G, Smith K. Indoor air pollution. In: Jamison DT, Breman JG, Measham AR, Alleyne G, Claeson M, Evans DB, Jha P, Mills A, Musgrove P, editors. Disease control priorities in developing countries. 2nd ed. Washington DC: The World Bank; 2006. p. 793–815.
Carter EM, Shan M, Yang X, Li J, Baumgartner J. Pollutant emissions and energy efficiency of Chinese gasifier cooking stoves and implications for future intervention studies. Energy Sustain Dev 2014;48(11):6461–7. http://dx.doi.org/10.1021/es405723w.
Chiang R, Farr K. Stove testing update — Release of Water Boiling Test protocol 4.2.3. Online; 2014 [http://www.cleancookstoves.org/blog/release-wbt-protocol-4-2-3.html, accessed June 23, 2014].
Churchill SW, Chu HHS. Correlating equations for laminar and turbulent free convection from a vertical plate. Int J Heat Mass Transfer 1975;18(11):1323–9. http://dx.doi.org/10.1016/0017-9310(75)90243-4.
Coovattanachai N. Biomass gasification research and field developments by the Prince of Songkla University, Thailand. Biomass 1989;18(3–4):241–71. http://dx.doi.org/10.1016/0144-4565(89)90036-X.
DeFoort M, L'Orange C, Kreutzer C, Lorenz N, Kamping W, Alders J. Stove manufacturers emissions and performance test protocol (EPTP). Technical Report. Engines and Energy Converesion Laboratory; Fort Collins; 2010. [Retrieved from http://www.cleancookstoves.org/our-work/standards-and-testing/learn-about-testing-protocols/protocols/downloads/eptp-protocol.pdf].
Goldemberg J, Johansson TB, Reddy AKN, Williams RH. A global clean cooking fuel initiative. Energy Sustain Dev 2004;8(3):5–12. http://dx.doi.org/10.1016/S0973-0826(08)60462-7.
Incropera FP, DeWitt DP, Bergman TL, Lavine AS. Fundamentals of heat and mass transfer. 6th ed. Hoboken: John Wiley and Sons; 2007.
ISO International Workshop on Clean and Efficient Cookstoves. Online http://www.pciaonline.org/files/ISO-IWA-Cookstoves.pdf, 2012. [accessed February 25, 2014].
Jetter JJ, Kariher P. Solid-fuel household cook stoves: characterization of performance and emissions. Biomass Bioenergy 2009;33(2):294–305. http://dx.doi.org/10.1016/j.biombioe.2008.05.014.
Jetter J, Zhao Y, Smith KR, Khan B, Yelverton T, DeCarlo P, et al. Pollutant emissions and energy efficiency under controlled conditions for household biomass cookstoves and implications for metrics useful in setting international test standards. Environ Sci Tech 2012;46(19):10827–34. http://dx.doi.org/10.1021/es301693f.
Kar A, Rehman IH, Burney J, Puppala SP, Suresh R, Singh L, et al. Real-time assessment of black carbon pollution in Indian households due to traditional and improved biomass cookstoves. Environ Sci Tech 2012;46(17):2993–3000. http://dx.doi.org/10.1021/es303338u.
L'Orange C, DeFoort M, Willson B. Influence of testing parameters on biomass stove performance and development of an improved testing protocol. Energy Sustain Dev 2012;16(1):3–12. http://dx.doi.org/10.1016/j.esd.2011.10.008.
Lin JL, Keener HM, Essenhigh RH. Pyrolysis and combustion of corn cobs in a fluidized bed: measurement and analysis of behavior. Combust Flame 1995;100(1–2):271–82. http://dx.doi.org/10.1016/0010-2180(94)00143-G.
MacCarty N, Still D, Ogle D. Fuel use and emissions performance of fifty cooking stoves in the laboratory and related benchmarks of performance. Energy Sustain Dev 2010;14(3):161–71. http://dx.doi.org/10.1016/j.esd.2010.06.002.
Mukunda HS, Dasappa S, Paul PJ, Rajan NKS, Yagnaraman M, Kumar DR, et al. Gasifier stoves — science, technology and field outreach. Curr Sci 2010;98(5):627–38.
Naeher LP, Smith KR, Leaderer BP, Mage D, Grajeda R. Indoor and outdoor $PM_{2.5}$ and CO in high- and low-density Guatemalan villages. J Expo Anal Environ Epidemiol 2000;10(6):544–51.
Northcross A, Chowdhury Z, McCracken J, Canuz E, Smith KR. Estimating personal PM2.5 exposures using CO measurements in Guatemalan households cooking with wood fuel. J Environ Monit 2010;12(4):873–8.
Quaak P, Knoef H, Stassen H. Energy from biomass: a review of combustion and gasification technologies. Technical report WTP422. Washington DC: The World Bank; 1999.
Reed TB, Larson R. A wood-gas stove for developing countries. Energy Sustain Dev 1996;3(2):34–7. http://dx.doi.org/10.1016/S0973-0826(08)60589-X.
Rehfuess E, Mehta S, Prüss-Üstün A. Assessing household solid fuel use: multiple implications for the millennium development goals. Environ Health Perspect 2006;114(3):373–8.
Rocky Mountain Pellet Company, Inc. Online http://www.rockymountainpellets.com, 2012. [accessed March 24, 2012].
Smith KR, Peel JL. Mind the gap. Environ Health Perspect 2010;118(12).
The Water Boiling Test: Version 4.2.3. Online http://www.cleancookstoves.org/our-work/standards-and-testing/learn-about-testing-protocols/protocols/downloads/wbt-protocol.pdf, 2014. [accessed June 23, 2014].
Tian L, Lan Q, Yang D, He X, Yu ITS, Hammond SK. Effect of chimneys on indoor air concentrations of PM10 and benzo[a]pyrene in Xuan Wei, China. Atmos Environ 2009;43(21).
Wendelbo P. The Peko Pe biomass household energy program. Online. http://wendelborecho.wordpress.com/2012/05/10/downloads, 2012. [accessed February 25, 2014].
Wisdom Innovations. Malaika Jiko user manual. Online. http://www.wisdomstoves.org/assets/photos/malaikamanual.pdf, 2013. [accessed February 28, 2014].